

Polaron morphologies in $\text{SrFe}_{1-x}\text{Ti}_x\text{O}_{3-\delta}$

H.D. Zhou and J.B. Goodenough*

Texas Materials Institute, ETC 9.102, 1 University Station, Code C2201, University of Texas at Austin, Austin, TX 78712-1063, USA

Received 23 October 2003; received in revised form 30 December 2003; accepted 16 January 2004

Abstract

The morphologies of the charge carriers in the perovskite system $\text{SrFe}_{1-x}\text{Ti}_x\text{O}_{3-\delta}$ are explored by transport and magnetic measurements. Oxygen vacancies are present in all samples, but they do not trap out the Fe^{3+} ions they introduce. The $x = 0.05$ composition was prepared with three different values of δ . They all show small-polaron conduction above 225 K; but where there is a ratio $c = \text{Fe}^{4+}/\text{Fe} < 0.5$, the polaron morphology appears to change progressively with decreasing temperature below 225 K to two-Fe polarons that become ferromagnetically coupled in an applied magnetic field at lower temperatures; With an applied field of 2500 Oe, divergence of the paramagnetic susceptibility for zero-field-cooled and field-cooled samples manifests a greater stabilization of ferromagnetic pairs on cooling in the applied field. With a $c > 0.5$, the data are consistent with a disproportionation reaction $2\text{Fe}^{4+} = \text{Fe}^{3+} + \text{Fe}(\text{V})\text{O}_{6/2}$ that inhibits formation of two-Fe polarons and, on lowering the temperature, creates $\text{Fe}^{3+}-\text{Fe}(\text{V})-\text{Fe}^{3+}$ superparamagnetic clusters.

© 2004 Elsevier Inc. All rights reserved.

Keywords: Perovskite; Polaron; Two-Fe polaron; Disproportionation

1. Introduction

The $\text{Fe}^{4+}/\text{Fe}^{3+}$ mixed-valent perovskites $R_{1-x}A_x\text{FeO}_3$ (R = rare earth elements, A = alkaline-earth elements) have been studied extensively. Of particular interest has been the $\text{La}_{1-x}\text{Sr}_x\text{FeO}_3$ system. In SrFeO_3 the high-spin Fe^{4+} ions have localized π -bonding 3d electrons in a t^3 manifold with spin $S = 3/2$ and an itinerant σ -bonding 3d electron in a σ^* band of e -orbital parentage. Whereas the de Gennes double exchange interaction between nearest neighbors is ferromagnetic, a ferromagnetic spiral–spin configuration with $q||[111]$ is formed [1,2] below a $T_N = 139$ K. LaFeO_3 , on the other hand, has a localized, high-spin Fe^{3+} : t^3e^2 configuration, and antiferromagnetic superexchange interactions between nearest neighbors give Type-G antiferromagnetic order below a $T_N = 750$ K [3,4]. Because the high-spin $\text{Fe}(\text{IV})/\text{Fe}(\text{III})$ redox couple lies near the top of the $\text{O}:2p^6$ bands, it contains a large $\text{O}-2p_\sigma$ component. Consequently, the holes that are initially introduced into LaFeO_3 by Sr^{2+} substitutions for La^{3+} prefer to occupy

molecular orbitals (MOs) rather than a localized e orbital; in fact, they tend to be trapped as pairs within an $\text{Fe}(\text{V})\text{O}_{6/2}$ MO complex as a result of the disproportionation reaction $2\text{Fe}^{4+} = \text{Fe}^{3+} + \text{Fe}(\text{V})\text{O}_{6/2}$. Mössbauer spectra have revealed the presence of Fe^{3+} and $\text{Fe}(\text{V})$, but not Fe^{4+} [5]. On the other hand, the initial electrons introduced into SrFeO_3 by substitution of La^{3+} for Sr^{2+} tend to be either itinerant or large polarons that repel one another by Coulomb forces. The $x = 2/3$ composition $\text{LaSr}_2\text{Fe}_3\text{O}_9$ has been identified to undergo charge ordering. Battle et al. [6] reported and Matsuno et al. [7] confirmed that, below a first-order transition at 198 K, $\text{Fe}(\text{V})\text{O}_{6/2}$ complexes order into every third (111) plane to give a CDW/SDW propagating along the [111] direction with a $q_{\text{SDW}} = 2q_{\text{CDW}}$ in the formal valence configuration ...353353... with spin ordering... $\uparrow\uparrow\uparrow\downarrow\downarrow\downarrow\dots$

An alternative way to introduce mixed $\text{Fe}^{4+}/\text{Fe}^{3+}$ valences is by the introduction of oxygen vacancies into SrFeO_3 , and substitution of Ti, Sn, and Zr for Fe has been shown to yield $\text{SrFe}_{1-x}\text{Ti}_x\text{O}_{3-\delta}$ [8], $\text{SrFe}_{1-x}\text{Sn}_x\text{O}_{3-\delta}$ [9], and $\text{SrFe}_{1-x}\text{Zr}_x\text{O}_{3-\delta}$ [10]; it had not been possible to attain oxygen stoichiometry in these perovskites even by annealing under an oxygen pressure $p\text{O}_2 = 60$ MPa [11]. The coexistence of antiferromagnetic

*Corresponding author. Fax: 512-471-7681.

E-mail address: jgoodenough@mail.utexas.edu
(J.B. Goodenough).

$\text{Fe}^{3+}\text{-O-Fe}^{3+}$ and ferromagnetic $\text{Fe}^{3+}\text{-O-Fe}^{4+}$ or $\text{Fe}^{3+}\text{-O-Fe(V)}$ interactions creates spin-glass behavior in $\text{SrFe}_{1-x}\text{Ti}_x\text{O}_{3-\delta}$ and $\text{SrFe}_{1-x}\text{Sn}_x\text{O}_{3-\delta}$. However, the role of trapping of Fe^{3+} ions by oxygen vacancies and the possibility of forming either two-Fe polarons or $\text{Fe(V)O}_{6/2}$ complexes in these compounds has not previously been investigated. In this paper, we report magnetic and transport data for $\text{SrFe}_{1-x}\text{Ti}_x\text{O}_{3-\delta}$ samples that were designed to address these issues.

2. Experimental

Polycrystalline samples of the system $\text{SrFe}_{1-x}\text{Ti}_x\text{O}_{3-\delta}$ ($0 < x < 1$) were prepared by standard solid-state reaction. Stoichiometric mixtures of SrCO_3 , Fe_2O_3 , and TiO_2 were ground and calcined in air at 1100°C for 24 h. The samples were then reground, pelletized, and sintered at 1100°C for another 24 h in air and cooled to room temperature.

Iodometric titration was used to determine the concentration δ of oxygen vacancies per formula unit; the sample stoichiometries are listed in Table 1 along with the fraction of iron atoms that are formally present as Fe^{4+} . Sample $x = 0.05$ was then annealed in air at 310°C for 12 h and in oxygen at 260°C for 12 h; the amounts of oxygen absorbed during these two processes were determined by thermogravimetric analysis (TGA).

Powder X-ray diffraction (XRD) patterns were recorded with a Philips PW 1729 powder XRD equipped with a pyrolytic graphite monochromator and $\text{CuK}\alpha$ radiation (1.54059 Å); Si was the internal standard. Data were collected in steps of 0.020° over the range $20^\circ \leq 2\theta \leq 80^\circ$ with a count time of 15 s per step. Peak

profiles for the XRD data were fitted with the program JADE. All samples were single-phase to XRD.

Magnetic susceptibility measurements were made with a Quantum Design DC superconducting quantum interference device (SQUID) magnetometer with an external magnetic field of 2500 Oe after cooling in zero-field (ZFC) or cooling in the measuring field (FC). Before any measurements were made, the samples were heated to $T = 320\text{ K}$ to remove any previous magnetic history.

The thermoelectric power $\alpha(T)$ was obtained with a laboratory-built apparatus as described elsewhere [12]. The resistivity was measured by a four-probe technique.

3. Results and discussion

The as-prepared $x = 0.05$ sample was orthorhombic $Pbnm$, Fig. 1(a), with $a = 5.471(1)\text{ \AA}$, $b = 10.966(3)\text{ \AA}$, and $c = 7.713(1)\text{ \AA}$. Samples $0.1 \leq x \leq 0.9$ were all cubic as shown in Fig. 1(b) for $x = 0.1$; the cubic lattice parameter increased nearly linearly with x , Fig. 2, in accordance with Vegard's law and a larger Ti^{4+} ion. The absence of superlattice peaks shows that the Fe and Ti atoms are randomly distributed over the perovskite octahedral sites.

The thermoelectric power contains, in general, three contributions

$$\alpha(T) = \alpha_s + \alpha_t(T) + \delta\alpha(T), \quad (1)$$

Table 1
Oxygen vacancies (δ), fraction of Fe that are Fe^{4+} (c), and sample stoichiometry for the $\text{SrFe}_{1-x}\text{Ti}_x\text{O}_{3-\delta}$ system

x	δ	c (Fe^{4+}/Fe)	Sample stoichiometry
0.05	0.31(2)	0.35	$\text{SrFe}^{3+}_{0.62}\text{Fe}^{4+}_{0.33}\text{Ti}^{4+}_{0.05}\text{O}_{2.69(2)}$
0.05 ^a	0.225(3)	0.53	$\text{SrFe}^{3+}_{0.45}\text{Fe}^{4+}_{0.50}\text{Ti}^{4+}_{0.05}\text{O}_{2.775(3)}$
0.05 ^b	0.18(1)	0.62	$\text{SrFe}^{3+}_{0.36}\text{Fe}^{4+}_{0.59}\text{Ti}^{4+}_{0.05}\text{O}_{2.82(1)}$
0.10	0.25(1)	0.45	$\text{SrFe}^{3+}_{0.50}\text{Fe}^{4+}_{0.40}\text{Ti}^{4+}_{0.10}\text{O}_{2.75(1)}$
0.20	0.19(2)	0.53	$\text{SrFe}^{3+}_{0.38}\text{Fe}^{4+}_{0.42}\text{Ti}^{4+}_{0.20}\text{O}_{2.81(2)}$
0.30	0.16(1)	0.53	$\text{SrFe}^{3+}_{0.33}\text{Fe}^{4+}_{0.37}\text{Ti}^{4+}_{0.30}\text{O}_{2.84(1)}$
0.40	0.14(2)	0.53	$\text{SrFe}^{3+}_{0.28}\text{Fe}^{4+}_{0.32}\text{Ti}^{4+}_{0.40}\text{O}_{2.86(2)}$
0.50	0.09(3)	0.64	$\text{SrFe}^{3+}_{0.18}\text{Fe}^{4+}_{0.32}\text{Ti}^{4+}_{0.50}\text{O}_{2.91(3)}$
0.60	0.06(1)	0.70	$\text{SrFe}^{3+}_{0.12}\text{Fe}^{4+}_{0.28}\text{Ti}^{4+}_{0.60}\text{O}_{2.94(1)}$
0.70	0.05(2)	0.67	$\text{SrFe}^{3+}_{0.10}\text{Fe}^{4+}_{0.20}\text{Ti}^{4+}_{0.70}\text{O}_{2.95(2)}$
0.75	0.04(2)	0.68	$\text{SrFe}^{3+}_{0.08}\text{Fe}^{4+}_{0.17}\text{Ti}^{4+}_{0.75}\text{O}_{2.96(2)}$
0.80	0.035(3)	0.65	$\text{SrFe}^{3+}_{0.07}\text{Fe}^{4+}_{0.13}\text{Ti}^{4+}_{0.80}\text{O}_{2.965(3)}$
0.90	0.02(1)	0.60	$\text{SrFe}^{3+}_{0.04}\text{Fe}^{4+}_{0.06}\text{Ti}^{4+}_{0.90}\text{O}_{2.98(1)}$

^a $x = 0.05$ sample annealed in air at 310°C for 12 h.

^b $x = 0.05$ sample annealed in oxygen at 260°C for 12 h.

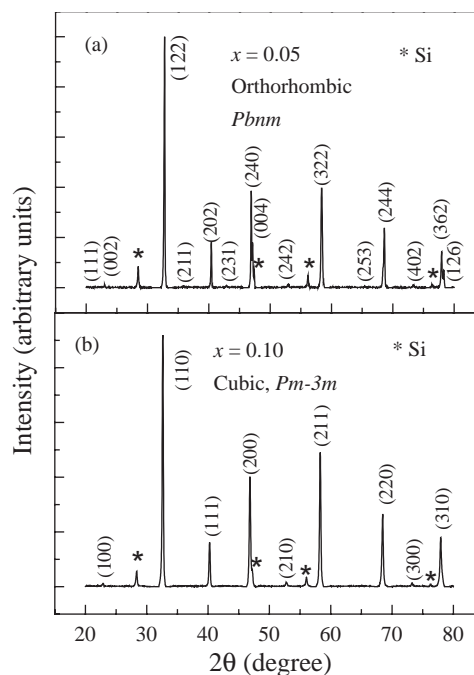


Fig. 1. Room temperature X-ray diffraction patterns for: (a) $x = 0.05$ (as prepared), and (b) $x = 0.1$ samples.

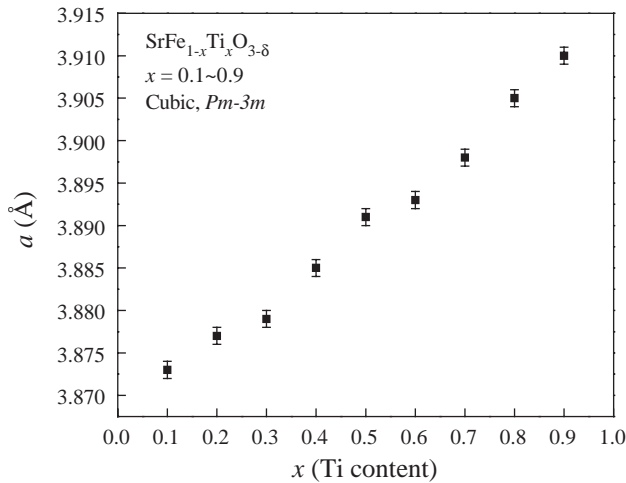


Fig. 2. Room temperature lattice parameters a for $\text{SrFe}_{1-x}\text{Ti}_x\text{O}_{3-\delta}$ with $0.1 \leq x < 1$.

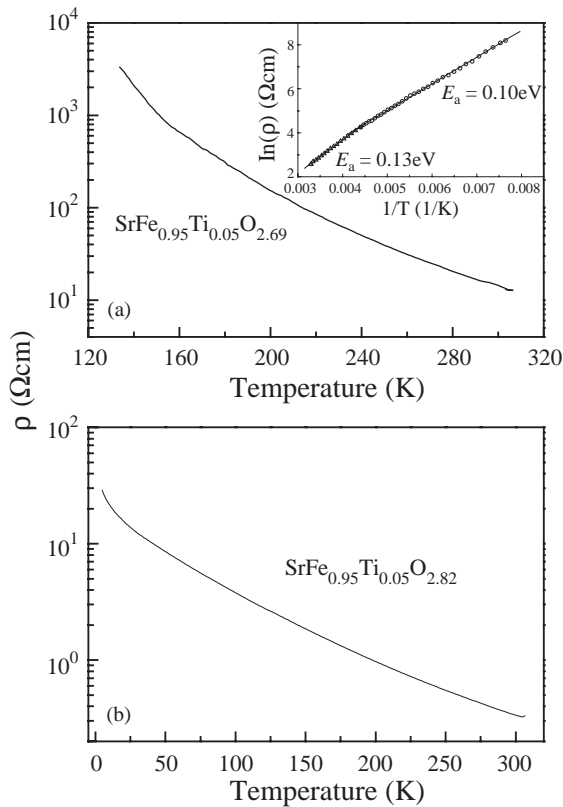


Fig. 3. Temperature dependences of resistivity ρ for: (a) $\text{SrFe}_{0.95}\text{Ti}_{0.05}\text{O}_{2.69}$ and (b) $\text{SrFe}_{0.95}\text{Ti}_{0.05}\text{O}_{2.82}$. Inset of (a): the $\ln \rho \sim 1/T$ curve for $\text{SrFe}_{0.95}\text{Ti}_{0.05}\text{O}_{2.69}$, symbols are experiment data, lines are fitting results.

where α_s is a statistical term that is temperature-independent for a fixed fraction of mobile charge carriers on available lattice sites, $\alpha_t(T)$ is a transport term that is relatively small for polaronic conduction, and $\delta\alpha(T)$ is a low-temperature enhancement that may be present with itinerant electrons. The resistivity data

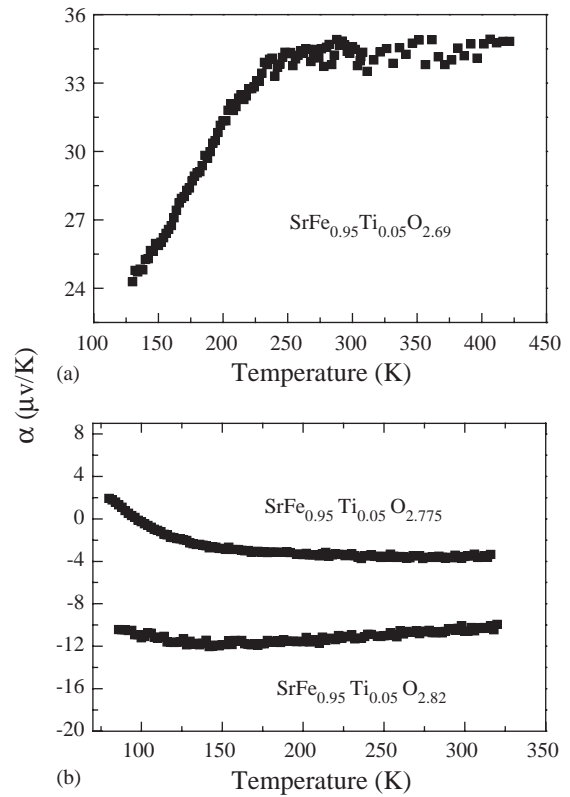


Fig. 4. Temperature dependences of thermoelectric power α for: (a) $\text{SrFe}_{0.95}\text{Ti}_{0.05}\text{O}_{2.69}$ (as prepared) and (b) $\text{SrFe}_{0.95}\text{Ti}_{0.05}\text{O}_{2.775}$ (annealed in air) and $\text{SrFe}_{0.95}\text{Ti}_{0.05}\text{O}_{2.82}$ (annealed in oxygen).

of Fig. 3 for as-prepared and O_2 -annealed $x = 0.05$ show an activated conduction, and the thermoelectric power $\alpha(T)$ is temperature-independent above 225 K, Fig. 4. These data show that the charge carriers are polarons, and the activation energy in the resistivity above 225 K, $E_a = 0.13$ eV, represents the polaron motional enthalpy entering the mobility $\mu_{\text{hop}} \propto \exp(-E_a/kT)$. Measurement was restricted to $T < 425$ K because TGA showed the sample begins to absorb oxygen from the air above 425 K. All the samples we investigated were polaronic conductors, so the statistical term dominates the thermoelectric power

$$\alpha_s = (k/e) \ln[\beta(1 - Qc)/Qc], \quad (2)$$

where k is the Boltzmann constant, e the charge of the mobile polarons, the spin-degeneracy factor is $\beta = 1$ due to strong intraatomic exchange, c the fraction of Fe atoms that have the formal valence Fe^{4+} , and Q the polaron size [13].

The as-prepared sample $\text{SrFe}_{0.95}\text{Ti}_{0.05}\text{O}_{2.69}$ would have an Fe^{4+} fraction $c = 0.33/0.95 = 0.35$ if all the Fe atoms are available to the holes, i.e., no trapping of electrons as Fe^{3+} ions at the oxygen vacancies. With this value of c , we calculated a $Q \approx 1$ from the temperature-independent part of $\alpha(T)$ above 225 K. A $Qc = 0.35 < 0.5$ corresponds to p-type charge carriers. Annealing the $x = 0.05$ sample in air and O_2 lowers the oxygen-

vacancy parameter δ . For the sample annealed in air, $\text{SrFe}_{0.95}\text{Ti}_{0.05}\text{O}_{2.775}$, $c = 0.50/0.95 = 0.53 > 0.5$ gives a small, temperature-independent $\alpha(T) < 0$ above 225 K as expected for $Q = 1$. Similarly, the oxygen-annealed sample with $\delta = 0.18$ has a $c = 0.62$, and an $\alpha(T) < 0$ of larger magnitude is again consistent with a $Q = 1$.

More interesting is the behavior of $\alpha(T)$ below 225 K. In the as-prepared sample, a drop in $\alpha(T) > 0$ on cooling below 225 K signals an increase in Qc , which can mean either an increase in c due to a trapping of mobile electrons, i.e., of Fe^{3+} ions at oxygen vacancies, or an increase in Q due to the condensation of two-Fe polarons. An oxygen vacancy has a lattice charge of 2+, which means that it can trap out Fe^{3+} ions above 225 K. On the other hand, ferromagnetic coupling between an $\text{Fe}^{3+}\text{--O--Fe}^{4+}$ pair could stabilize a superparamagnetic two-Fe polaron in which the electron of the $\text{Fe}^{4+}/\text{Fe}^{3+}$ couple occupies a MO; fast electron transfer between the iron pair would give ferromagnetic coupling via double exchange. The formation of MOs within an $\text{Fe}^{3+}\text{--O--Fe}^{4+}$ pair would increase Q and lower $\alpha(T)$; ferromagnetic coupling within two-Fe polarons would increase the paramagnetic susceptibility. The paramagnetic susceptibility should distinguish between these two possible models for lowering $\alpha(T)$ with decreasing temperature below 225 K in the as-prepared sample.

The molar and inverse molar magnetic susceptibilities χ_{mol} and $1/\chi_{\text{mol}}$ for the three $x = 0.05$ samples are shown in Fig. 5. For the ZFC susceptibility of the as-prepared sample with $\delta = 0.31$, a Curie–Weiss law above 225 K extrapolates to a Weiss constant $\theta = -115$ K, and a maximum at a $T_{\text{N}} = 25$ K signals antiferromagnetic coupling in a percolating matrix. The strong $\text{Fe}^{3+}\text{--O--Fe}^{3+}$ antiferromagnetic superexchange interactions are dominant. However, below a $T^* = 220$ K in $\text{SrFe}_{0.95}\text{Ti}_{0.05}\text{O}_{2.69}$, the ZFC and FC susceptibilities diverge, which indicates a greater stabilization below $T < 220$ K in the FC than in the ZFC runs of ferromagnetic coupling within the two-Fe polarons in a field of $H = 2500$ Oe. Trapping out of Fe^{3+} ions at oxygen vacancies would not alter the magnetic susceptibility. Moreover, a smaller activation energy for the charge-carrier mobility below 225 K, see inset of Fig. 3(a), is consistent with formation of two-Fe polarons. Trapping of the charge carriers would increase the activation energy of the resistivity.

Extension of the model of ferromagnetic two-Fe polarons to the more oxidized $x = 0.05$ samples runs into problems. The magnitude of the $\alpha(T) < 0$ for the air-annealed sample with $\delta = 0.225$ does not increase with decreasing temperature below 225 K, as would be expected for an increase of Qc ; rather, $\alpha(T)$ increases, becoming positive at lower temperature, which signals a decrease in Qc from 0.53 to a value less than 0.5. Some

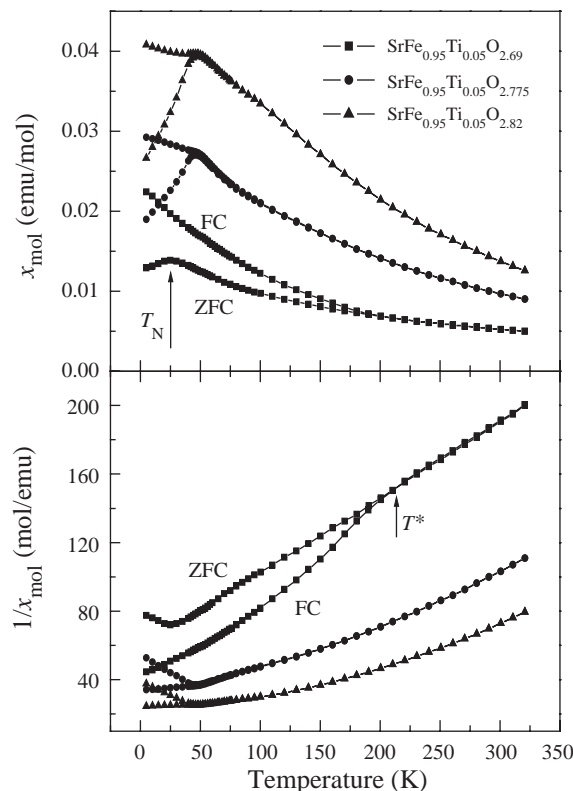


Fig. 5. Molar magnetic susceptibility χ_{mol} and their inverse $1/\chi_{\text{mol}}$ of $x = 0.05$ samples.

other mechanism must be operative in this sample, which has a higher Fe^{4+} -ion concentration. Since the $\text{Fe}^{4+}\text{--O--Fe}^{4+}$ and $\text{Fe}^{3+}\text{--O--Fe}^{4+}$ interactions are ferromagnetic by vibronic superexchange associated with the $\text{Fe}^{4+}: t^3e^1$ Jahn–Teller ions, the high-temperature Curie–Weiss law extrapolates to a Weiss constant $\theta > 0$ where a $c \geq 0.5$ exists. Coulomb forces minimize the $\text{Fe}^{3+}\text{--O--Fe}^{3+}$ interactions. Below room temperature, the $1/\chi_{\text{mol}}(T)$ curves show evidence of considerable short-range ferromagnetic order above a Néel temperature, T_{N} providing clear evidence for ferromagnetic clusters with a sufficient concentration of $\text{Fe}^{3+}\text{--O--Fe}^{3+}$ interactions to give an overall antiferromagnetic coupling. However, in the samples with $c > 0.5$ there is no divergence of the ZFC and FC paramagnetic susceptibilities, which is also consistent with a failure to stabilize a substantial concentration ferromagnetic two-Fe pairs in a magnetic field because of the existence of a competing mechanism.

With $c > 0.5$, the Coulomb forces are not able everywhere to keep separate two Fe^{4+} ions, so there will be some $\text{Fe}^{4+}\text{--O--Fe}^{4+}$ interactions. Experiments on the $\text{La}_{1-x}\text{Sr}_x\text{FeO}_3$ system have shown that where these interactions are present, a disproportionation reaction $2\text{Fe}^{4+} = \text{Fe}^{3+} + \text{Fe(V)}\text{O}_{6/2}$ occurs. This reac-

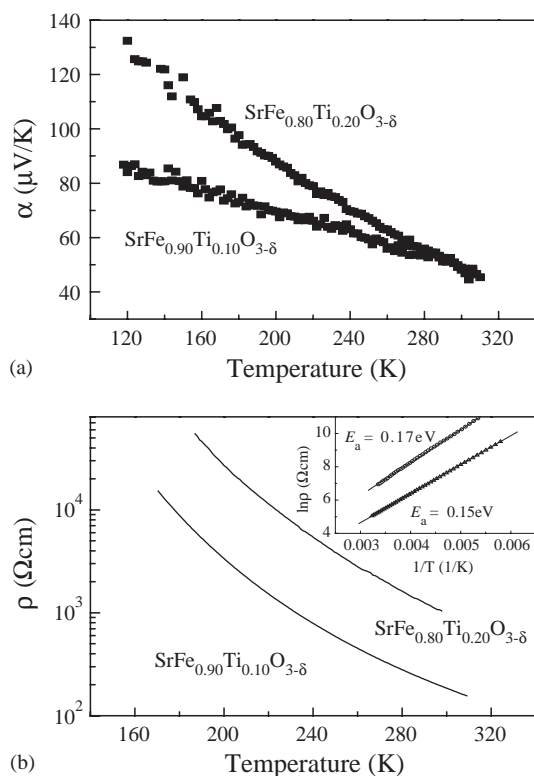


Fig. 6. Temperature dependences of: (a) thermoelectric power α and (b) resistivity ρ for $x = 0.1$ and 0.2 samples. Inset of (b): the $\ln \rho \sim 1/T$ curves for $x = 0.1$ and 0.2 , symbols are experiment data, lines are fitting results.

tion would decrease the c for mobile Fe^{4+} ions, inhibit stabilization of two-Fe $\text{Fe}^{3+}\text{--O--Fe}^{4+}$ pairs, and introduce $\text{Fe}^{3+}\text{--O--Fe}^{3+}$ interactions to provide anti-ferromagnetic coupling between ferromagnetic $\text{Fe}^{3+}\text{--Fe(V)--Fe}^{3+}$ clusters as in $\text{LaSr}_2\text{Fe}_3\text{O}_9$. A similar mechanism would be operative in the annealed samples, but how the formation of the ferromagnetic clusters would impact Qc is not evident as the ferromagnetic clusters may not be mobile.

Fig. 6 shows the $\alpha(T)$ and $\rho(T)$ data for the as-prepared samples $x = 0.1$ and 0.2 . If the Fe^{4+} ions were all present as mobile small polarons, an $\alpha(T) \approx 0$ that is temperature-independent should be observed. Instead, we find an $\alpha(T) > 0$, that increases nearly linearly with decreasing temperature, which is indicative of trapping out of mobile holes. According to our model, this trapping signals the disproportionation reaction $2\text{Fe}^{4+} = \text{Fe}^{3+} + \text{Fe(V)}\text{O}_{6/2}$. The susceptibility data, Fig. 7, show evidence of ferromagnetic two-Fe pairs below a T^* near 200 K in the $x = 0.1$ sample, but there is no divergence of the FC and ZFC paramagnetic susceptibilities in the $x = 0.20$ sample where there is evidence of more extensive disproportionation in this $c > 0.5$ sample.

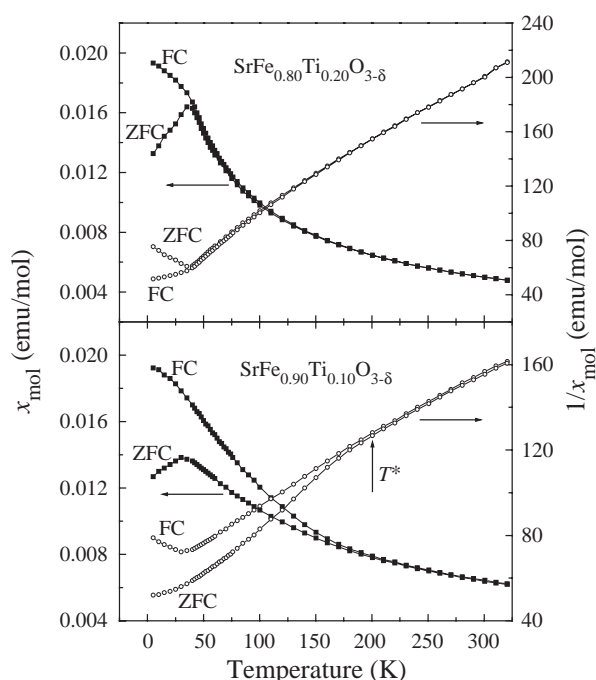


Fig. 7. Molar magnetic susceptibility χ_{mol} and their inverse $1/\chi_{\text{mol}}$ of $x = 0.1$ and 0.2 samples.

4. Conclusions

From our measurements of the transport and magnetic properties of the system $\text{SrFe}_{1-x}\text{Ti}_x\text{O}_{3-\delta}$, we draw the following conclusions:

- (1) For an Fe^{4+}/Fe ratio less than 0.5, the electrons of the $\text{Fe}^{4+}/\text{Fe}^{3+}$ redox couple remain localized as mobile small polarons that have access to the Fe atoms neighboring an oxygen vacancy, but below 225 K, two-Fe pairs are formed that become coupled ferromagnetically in an applied magnetic field; stabilization of the ferromagnetic coupling is greater in FC than in ZFC samples, and the concentration of the ferromagnetic pairs vanishes above T^* in the FC samples.
- (2) For an Fe^{4+}/Fe ratio greater than 0.5, a disproportionation reaction $2\text{Fe}^{4+} = \text{Fe}^{3+} + \text{Fe(V)}\text{O}_{6/2}$ is stabilized below a temperature that increases with the ratio Fe^{4+}/Fe . The Fe(V) atoms suppress $\text{Fe}^{3+}\text{--O--Fe}^{4+}$ pairs and form superparamagnetic clusters. Similar $\text{Fe}^{3+}\text{--Fe(V)--Fe}^{3+}$ ferromagnetic clusters have been found in $\text{LaSr}_2\text{Fe}_3\text{O}_9$.
- (3) This unusual behavior is made possible by the strong covalent mixing of $\text{O--}2p_\sigma$ character into the $\text{Fe}^{4+}/\text{Fe}^{3+}$ redox energy, which lies close to the top of the $\text{O}^{2-}:2p^6$ bands; the covalent mixing puts the $\text{Fe}^{4+}/\text{Fe}^{3+}$ redox band at the crossover from localized to itinerant electronic behavior, which is a first-order transition.

Acknowledgments

The authors are grateful to Dr. R.I. Dass for helpful discussions, and to the National Science Foundation and the Robert A. Welch Foundation of Houston, Texas, for financial support.

References

- [1] P.K. Gallagher, J.B. McChesney, D.N.E. Buchanan, *J. Chem. Phys.* 41 (1964) 2429.
- [2] T. Takeda, S. Komura, M. Fugii, *J. Magn. Magn. Mater.* 31–34 (1983) 797.
- [3] W.C. Koehler, E.O. Wollan, *J. Phys. Chem. Solid.* 2 (1957) 100.
- [4] W.C. Koehler, E.O. Wollan, M.K. Wilkinson, *Phys. Rev.* 118 (1960) 58.
- [5] S.E. Dann, D.B. Currie, M.T. Weller, M.F. Thomas, A.D. Al-Rawwas, *J. Solid State Chem.* 109 (1994) 134.
- [6] P.D. Battle, T.C. Gibb, S. Nixon, *J. Solid State Chem.* 79 (1989) 75.
- [7] J. Matsuno, T. Mizokawa, A. Fujimori, K. Mamiya, Y. Takeda, S. Kawasaki, M. Takano, *Phys. Rev. B.* 60 (1999) 4605.
- [8] T.C. Gibb, P.D. Battle, S.K. Bollen, R.J. Whitehead, *J. Mater. Chem.* 2 (1992) 111.
- [9] K.S. Roh, K.H. Ryu, C.H. Yo, *J. Solid State Chem.* 142 (1999) 288.
- [10] M. Wyss, A. Reller, H.R. Oswald, *Solid State Ionics.* 101–103 (1997) 547.
- [11] P. Adler, S. Eriksson, *Z. Anorg. Allg. Chem.* 626 (2000) 118.
- [12] J.B. Goodenough, J.-S. Zhou, J. Chen, *Phys. Rev. B.* 47 (1993) 5275.
- [13] J.B. Goodenough, *J. Solid State Chem.* 1 (1970) 349.